Chapter 10
Analysis of the Potential Metal Hydrides for Hydrogen Storage in Automobile Applications

Dosawada Pavan Sai, Niraj Kumar, and Vishal Saxena

Abstract Considering the increase in air pollution and depletion of the available fossil fuels there is a need for the implementation of other energy sources for industrial use and automobiles. Hydrogen fuel is considered as the possible solution to act as a new energy source. It is the ideal means for energy storage for automobiles as it leads to zero emissions in case it is used in fuel cells. Unlike electrical vehicles the hydrogen fuel cells offer advantage of fast recharging and at present there are lot of technologies available which can make the hydrogen production easy and economical in future. However, the wide spread of hydrogen is restricted due its storage as the boiling point of hydrogen is 20.4 K at 1 atm. Thus, the storage of hydrogen in liquid form requires higher pressures and cryogenic conditions which consumes external energy. In addition, storing hydrogen in gaseous form is not feasible as it requires higher volumes. Storing hydrogen in the form of metal hydrides requires hydrogen to react with other metals and it can be released whenever required by breaking bond. Thus, metal hydrides have potential to overcome the problems associated with storage and has many advantages such as thermal stability, automobile safety, no fuel losses and long-term storage, etc. However, lower gravimetric storage density is a major issue beside it requires external source for hydrogen release. According to present automobile manufacturing requirement, the ultimate hydrogen storage material should have high gravimetric reversibility preferably greater than 10wt % of hydrogen, high reversibility which should be greater than 1500 cycles. Many metal hydrides with the suitable catalyst or nanoparticles have shown tendency towards satisfying the above conditions. In the present study, thermodynamic and kinetics for every such metal hydride are mathematically analyzed using the equations based on pore size and surface area. By knowing the thermodynamic and kinetic requirements of metal hydride reactions the suitable material for the automobile can be predicted and the technologies required for the proper release of the hydrogen can be suggested.

Keywords Metal hydride · Hydrogen · Thermodynamic analysis

D. P. Sai · N. Kumar (✉)
Department of Mechanical Engineering, ASET, Amity University, Noida, India

V. Saxena
Department of Fuel (FMME) Engineering, I.I.T (ISM), Dhanbad, Jharkhand, India

10.1 Introduction

The decrease in availability of fossil fuels and the undesirable environmental impacts caused by them led to the initiative of using the most promising alternative fuels. In the search of such alternative fuels, one of the most advantageous and eco-friendly fuel found to be hydrogen (H_2) which has higher energy density compared to gasoline and unlike hydrocarbon fuels it won't release carbon emissions out. Hydrogen has 3 times higher energy content than gasoline. Lower heating values are 33.3 kWh/kg for hydrogen and 11.1 kWh/kg for gasoline. Hydrogen is not freely available on the earth surface but it can be generated through many methods such as thermochemical process which use energy in sources like natural gas, coal, or biomass to release hydrogen from their molecular structures, electrolytic processes which use electricity to split water into hydrogen and oxygen, direct solar water splitting where the radiant light energy is used to split water into hydrogen and oxygen and biological processes where bacteria and microalgae can produce hydrogen through biological reactions using sunlight and organic matter. All these methods are in research phase and there is lot of advancements required to make hydrogen available at low cost and without any scarcity (Kumar 2019).

The main challenge in utilization of hydrogen as fuel is the difficulty in its storage. Hydrogen has a boiling point of $-252.9\,°C$ at 1 atm. In-order to store the hydrogen in liquid form we need to provide the cryogenic temperatures or the higher pressures to increase its boiling point. Storing of hydrogen in gaseous form requires higher volume and pressure containers which will also post a major challenge in automobile application. The various targets set for hydrogen storage for the year 2020 and 2025 are shown in Table 10.1. To overcome the limitations of liquid and gaseous hydrogen storage, researchers are focusing on chemical storage of hydrogen within the suitable materials. Hydrogen storage material includes complex metal hydrides, metal hydrides, chemical hydrides, carbon nanotubes, inorganic nano tubes and sorbents such as metal organic frameworks.

Table 10.1 DOE Targets for hydrogen storage systems for on-board vehicular applications (Schneemann et al. 2018)

Storage parameters	Units	2020	2025	Ultimate
System gravimetric capacity:	kWh kg^{-1} (wt%)	1.5 (4.5)	1.8 (5.5)	2.5 (6.5)
Volumetric capacity: usable energy density from H_2	kWh L^{-1} (kg H_2 L^{-1})	1.0 (0.03)	1.3 (0.04)	1.7 (0.05)
Min/max delivery temperature	°C	−40/85	−40/85	−40/85
Cyclelife (uptake/release cycles)	Cycles	1500	1500	1500
Delivery pressure	bar (abs)	5	5	5
System fill time	Min	3–5	3–5	3–5
Fuel purity (H_2 from storage)	% H_2	99.97	99.97	99.97

According to the bond formation, the hydrogen storage materials are classified in three categories such as physisorption materials, off board regenerable hydrides and on-board reversible hydrides. Physisorption is the adsorption process in which the forces involved are interatomic forces. These materials include metal–organic frameworks, organic polymers, porous carbons and zeolites. H_2 is physiosorbed on the surface of the pores where the storage capacity majorly depends on the surface area and pours volume. The use of physisorption materials in hydrogen storage systems is limited due to its weak Van-der wall forces. The main advantage of these materials in their fast desorption and adsorption kinetics.

Chemisorption is the adsorption that is related to the strong chemical bond formed between the adsorbate and adsorbent molecules. Off-board regenerable hydrides and On-board reversible hydrides comes under this category. Materials like covalently bound metal hydrides, metal hydrides, borohydrides and metal amides come under the category of on-board reversible hydrides. In these materials the hydrogen is released by breaking the chemical bond by endothermic reactions which generally takes place in reasonable temperature and pressure.

Off-board regenerable hydrides store hydrogen in the form of covalently bound hydrogen materials which release hydrogen exothermally. It involves complex chemical process which limited its use in onboard vehicle hydrogen storage. Some of the materials are ammonia borane and hydrocarbons.

In the present study, the metal hydrides with potential hydrogen storage properties were briefly mentioned. The report gives the details about types of metal hydrides available and their gravimetric capacity, kinetic and thermal properties. Various methods are suggested to improve the performance of metal hydrides. The mathematical equations related to the thermodynamics of dehydration and hydration process in the metal hydrides is also shown.

10.2   Physisorption-Based Hydrogen Storage

The hydrogen storage is possible through two methods such as physisorption and chemisorption. In physisorption process the materials involved are metal organic frameworks, organic polymers, porous carbons and zeolites.

10.2.1   Metal Organic Frameworks (MOFs)

Metal organic frameworks (MOFs) are one of the promising materials for hydrogen storage. MOFs are originally crystalline materials which consists of metal ions linked together by various organic ligands which generate micro pores (2 nm) and channels. The frame topology, surface area and pore sizes can by readily modified by selecting the molecular building blocks. MOFs generally have permanent porosity, high specific surface area and defined structures. The highest excess hydrogen storage

capacity which was reported so far for MOFs is 99.5 mg g^{-1} at 56 bar and 77 K. The MOF-5 which is prepared from the materials, benzene-1, 4-dicarboxylate (BDC) and Zn (II) salt have shown 4.5 wt% at 77 K and 1.0 atm and 1.0 wt% at room temperature. The preparation and handling conditions have also affected the hydrogen uptake preparation and handling under nitrogen (N_2) atmosphere led to H_2 uptake of excess 7.1 wt% at 77 K and 40 bar. MOFs for hydrogen storage which were based on physisorption should have a combination of high specific surface area and small pores but these two will not be proportional. Materials with small pores often leads to a reduced specific surface area. To meet the U.S. DOE targets the highly stable MOFs with pore volume and surface area which has many open metal sites must be investigated (Suh et al. 2012).

10.2.2 Porous Carbons

For achieving the high-capacity hydrogen storage, porous carbon should possess low bulk density, highly accessible adsorption surface and strong hydrogen adsorption enthalpy. Various carbon materials such as carbon aerogels, activated carbon, carbon nano tubes, templated carbon, and graphene contain high surface area pores. The properties such as total pore volume, specific surface area, pore size, micropore surface area and micropore volume, can be tailored by relevant experimental parameters and proper synthesis methods (Saxena et al. 2021). The thermodynamics of porous carbon material H_2 binding can be improved by two strategies. The first approach is to increase the specific surface area of carbon with suitable pore width which may allow multiple adsorption layers to be formed. The second approach is doping with the light weight elements which helps to functionalize the porous carbon (Xia et al. 2013).

10.2.2.1 Carbon Nanotubes

Carbon nanotubes are basically cylindrical molecules which consists of rolled up sheets of single layered carbon atoms. Carbon nanotubes have lower surface area and pour volume than that of porous carbon. Therefore, the hydrogen storage capacities of carbon nano tubes are lower than 1 wt% at ambient temperature and 100 bars pressure. However, at cryogenic temperatures the storage capacity can be increased. H_2 uptake of 2.4 wt% at 77 K for purified single walled carbon nanotubes has been observed. In addition, single walled carbon nanotubes exhibit increased storage capacity from 1 to 1.7 wt% at 77 K and 1 bar after subjected to acid treatment. It has been reported that the single walled and multi walled carbon nano tubes can normally reversibly adsorb H_2 of 1.5 wt% per 1000 m^{2}g^{-1} under ambient conditions. According to the above observations we can conclude that the carbon nano tubes are not potential material for hydrogen storage at ambient conditions (Xia et al. 2013).

10.2.2.2 Activated Carbons

Activated carbon is a form of carbon processed to have small and low volume pores that increase the surface area available. The usually available specific surface area is up to 3000 m^2g^{-1} and with abundance of micropore size less than 1 nm. The experimental investigations on activated carbons demonstrated that H_2 uptake about 2.5 wt% at low pressure (1–40 bar) (Yamaura et al. 2002) and 5.5 wt% at high pressures up to 60 bar and 77 k were achievable (Dehouche et al. 1999). The highest gravimetric capacity for commercially available activated carbon is found to be 1 wt% at room temperature and at 700 bar pressure (Xia et al. 2013).

10.2.2.3 Carbon Aerogels

Carbon aerogels are the new class of activated carbons which has a specific surface area of 3200 m^2g^{-1}. They exhibit a maximum adsorption capacity of 5.3 wt% at 77 k and pressure of 20–30 bar. The hydrogen adsorption enthalpy of aerogels is found to be 7.0 kJ mol^{-1}. Hydrothermal carbonization of organic material followed by chemical activation with KOH can generate carbon materials with specific surface area of 2700 m^2g^{-1} and H_2uptake of 6.4 wt% at 77 k and 20 bar (Xia et al. 2013).

10.2.3 Zeolites

Adsorption of gases in Zeolites is a well-known phenomenon. The main principle is that the guest molecules are forced under elevated temperatures and pressures into the cavities of molecular host. Upon cooling to room temperatures, the hydrogen gets entrapped inside the cavities of zeolites. It can be released again by raising the temperatures. One of the major advantages of using zeolite as hydrogen storage material is their thermal and chemical stability. The use of different exchangeable cations will offer a different thermodynamic heat of adsorption which allows zeolites to be tuned to provide improved adsorption at elevated temperatures. The hydrogen uptake capacity of the zeolite like carbon material is among the highest ever reported for carbon or any other porous material. Zeolite templated porous carbon have shown a hydrogen storage capacity of 4.5 wt% at 20 bar and 77 K (Xia et al. 2013).

10.3   Chemisorption-Based Hydrogen Storage

10.3.1   *Complex Metal Hydrides*

Complex metal hydrides are the components composed of metal cations such as group 1 and 2 elements and hydrogen containing complex anions such as amides, borohydrides and alanates. Complex metal hydrides are of interest because of their light weight and high hydrogen storage capacities. They release hydrogen by heating or chemical reactions. Some of the complex hydrides have reported to release hydrogen even in presence of water or aqueous solution. Some of the intermetallic hydride combinations are shown in Table 10.2.

10.3.1.1   Metal Amides

The amide hydride composite hydrogen storage system has a general form of $M(NH_2)_xM'H_y$ where M refers to the metal and x and y refers to the valency of M. $LiNH_2$–LiH (lithium amide and lithium hydride composite) was the first amide identified which shown the possibility of storing the hydrogen at large quantities. In the chemical reaction between $LiNH_2$ (lithium amide) and LiH (lithium hydride), firstly one equivalent.H_2 and Li_2NH are formed (Wiberg and Amberg 1971). Then the both products will further react with LiH to form two equivalent H_2 and form Li_3N. In total 10.5 wt% of H_2 can be adsorbed/desorbed in the complete reaction (Gizer et al. 2020).

$$LiNH_2 + 2LiH \Leftrightarrow Li_2NH + LiH + H_2 \Leftrightarrow Li_3N + 2H_2 \qquad (10.1)$$
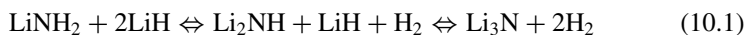
LiH is a highly stable hydride which has a formation enthalpy of −91 kJ/mol, desorbs hydrogen at the temperature higher than 600 °C. The decomposition of $LiNH_2$ takes place at low temperature of 300 °C. Therefore, the composite will release hydrogens at very low temperature which is less than 180 °C.

Table 10.2 Examples of intermetallic hydrides (Dornheim 2011)

S. No.	Composition	A	B	Compounds
1	A_2B	Mg, Zr	Ni, Co, Fe	Zr_2Fe, Mg_2Ni, Mg_2Co,
2	AB	Ti, Zr	Ni, Fe	TiFe, $TiNi_{,,}$ ZrNi
3	AB_2	Zr, Ti, Y, La	V, Cr, Mn, Fe, Li	YNi_2, $LaNi_2$, ZrV_2, YMn_2, $ZrCr_2$, $ZrMn_2$, $TiMn_2$
4	AB_3	La, Y, Mg	Ni, Co	$LaCo_3$, YNi_3, $LaMg_2NI_9$
5	AB_5	Ca, La, rare earth	Ni, Cu, Co, Pt, Fe	$LaNi_5$, $CeNi_5$, $CaNi_5$, $LaPt_5$, $LaFe_5$

H$_2$ release depends on the chemical interaction between the reactants. H$^{\partial+}$ and H$^{\partial-}$ have a high chemical potential which can be considered as one of the dehydrogenations driving forces. Many variations of amides are possible by matching the materials of H$^{\partial+}$ such as LiNH$_2$, with the materials of H$^{\partial-}$ such as LiH (lithium hydride), MgH$_2$ (magnesium hydride), Mg(BH$_4$)$_2$ (magnesium borohydride), LiBH$_4$ (lithium borohydride), LiAlH$_4$ (lithium aluminium hydride) which gives the amide composites. Mg(NH$_2$)$_2$–2LiH (magnesium amide and lithium hydride composite) have shown a gravimetric capacity of 5.6 wt% with high reversibility and hydrogen desorption at 1 bar pressure and temperature of 90 °C (Gizer et al. 2020).

Amide hydride hydrogen storage have many kinetic barriers which will be associated with the hydrogen dissociation, interface reactions, nucleation and diffusion process. Intensive ball milling of species such as LiNH$_2$–LiH and Mg(NH$_2$)$_2$–2LiH have shown a remarkable improvement in hydrogen storage due to the decrease in the particle size and increase in the homogenous distribution of reaction mixture. In the continuous rehydration and de-hydration, the small particles are prone to get aggregated into larger once which eventually slows down the reaction kinetics. Some of the methods such as introduction of proper dispersants which confine with scaffold materials can reduce the aggregate growth of reactant particles to some degrees. Some of the catalytic additives are identified which can improve the kinetic performance of amides. Catalytic effects of transition metals such as Fe, Co, Ni and Pt were significantly seen in amides. Introduction of multifunctional additives is required to improve the storage capacity and kinetics of amide hydrogen storage (Wang et al. 2013).

10.3.1.2   Borohydrides

Metal borohydride M(BH$_4$)$_n$ has a cation M^{n+} and an anion BH^{4-} in which B is covalently bonded with 4 hydrogen atoms. Borohydrides such as LiBH$_4$ (lithium tetrahydroborate), Mg(BH$_4$)$_2$ (magnesium borohydride) and Ca(BH$_4$)$_2$ (calcium borohydride) have shown the gravimetric capacity higher than 10 wt%.

Many metal borohydrides are found to be irreversible which limited their use in on-board applications. Research carried out on exploring the reversibility of lithium calcium and magnesium borohydrides. LiBH$_4$ is found to be reversible at higher temperatures of 600 °C. Ca and Mg borohydrides have shown reversibility at temperatures and pressures lower than lithium but they have some pre-assumed end products. Decreasing the dehydrogenation enthalpy is the major point of research in using the Li (lithium), Ca (calcium) and Mg (magnesium) borohydrides as the on-board hydrogen storage materials. Combining M(BH$_4$)$_n$ with other metals, metal hydrides and complex hydrides is the major approach to reduce the dehydrogenation enthalpy. 2LiBH$_4$–MgH$_2$ was the mostly studied element in this context (Lu et al. 2019). Pure LiBH$_4$ releases 13.8 mass% of hydrogen according to the reaction shown below.

$$LiBH_4 \leftrightarrow LiH + B + 3/2H_2 \qquad (10.2)$$

In this reaction the ΔH_{des} (change in enthalpy for dehydrogenation) is found to found to be 67 kJ/mol. The same reaction when carried out again with MgH_2 has shown the ΔH_{des} of 46 kJ/mol according to the following reaction.

$$2LiBH_4 + MgH_2 \leftrightarrow 2LiH + MgB_2 + 4H_2. \qquad (10.3)$$

This combination has shown the decrease in T_d (dehydrogenation temperature) along with the improvement in the kinetic performance of re-hydrogenation which improves the reversibility. But the pressure higher than 0.3 MPa is essential to supress the formation of $Li_2B_{12}H_{12}$ (Orimo et al. 2007).

Many additives such as metals, oxides, halides, and carbon-based materials when mixed with borohydrides have shown good performance in encountering the sluggish kinetics of metal borohydrides. In this regard adding $0.2MgCl_2$–$0.1TiCl_3$ (magnesium chloride and titanium chloride-based catalyst) into $LiBH_4$ have shown a super catalytic effect, releasing 5 mass% of hydrogen from 60 to 400 °C. Addition of $ZrCl_4$ into the $2LiBH_4$–MgH_2 has influenced its dehydrogenation kinetics and significantly reduced the incubation period of first dehydrogenation. Nanoconfinement is an approach which can improve the thermodynamics and kinetics of hydrogen storage materials. $LiBH_4$ which are nanoconfined to carbon scaffolds with a pore size of 13-nm has shown 50 times increase in dehydrogenation rates at a temperature of 300 °C and the capacity loss for 3 cycles is decreased from 72 to 40% compared to the bulk $LiBH_4$. Nano porous carbon with a smaller pore size of 2 nm can supress the release of B_2H_6 (Wang et al. 2013).

10.3.1.3   Metal Alanates

Metal alanates are also known as metal aluminium hydrides which contain metal cations and aluminium hydride anions. Alanates are moisture and air sensitive. The gravimetric capacities of alanates such as $LiAlH_4$ and $NaAlH_4$ are reported to be 10.6 wt% and 7.4 wt% respectively. One of the major metal alanate was found to be $LiAlH_4$ (lithium aluminium hydride). The equation which involves the dehydrogenation of $LiAlH_4$ is given as follows.

$$LiAlH_4 \Leftrightarrow 1/3Li_3AlH_6 + 2/3\ Al + H_2 \qquad (10.4)$$
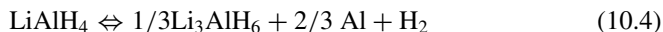
The $LiAlH_4$ undergo the phase transition at a temperature of 160–177 °C before it undergoes the above dehydrogenation reaction which occurs at 187–218 °C. This first dehydrogenation reaction was exothermic with ΔH (change in enthalpy) of -10 kJ/(mol of H_2). Then the second dehydrogenation reaction of Li_3AlH_6 takes place endothermically at 228–282 °C with ΔH of 25 kJ/(mol of H_2).

$$Li_3AlH_6 \Rightarrow 3LiH + Al + 3/2\ H_2 \qquad (10.5)$$
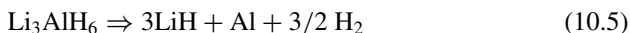
Then the LiH undergo dehydrogenation at 370–483 °C with ΔH of 140 kJ/mol.

Table 10.3 Storage data for low and high storage hydrides

S. No.	Material	Volume (l)	Weight (kg)	H$_2$ quantity stored (kg)	References
1	TiFe	50	200	4	Reilly and Wiswall (1974)
2	Mg$_2$Ni	50	100	4	Kohno et al. (1996)
3	MgH$_2$	50	100	8	Buchner (1978)

Doping of the LiAlH$_4$ with Ti (titanium) has enhanced the dehydrogenation kinetics. It was found that with 3 mol% addition of TiCl$_4$ (titanium tetrachloride) and 5 min of mechanical milling, the first dehydrogenation of LiAlH$_4$ into Li$_3$AlH$_6$ and aluminium will take place at room temperature. With 2 mol% addition of TiCl$_3$ in Li$_3$AlH$_6$, the decomposition into LiH and Al was found to be occurring at temperature as low as 100 °C (Orimo et al. 2007).

10.3.2   Metal Hydrides

Many metals form metal hydrides by reacting reversibly with hydrogen. The equation involved in formation of metal hydride is as follows:

$$Me + x/2H_2 \Leftrightarrow MeH_x + Q \tag{10.6}$$

Here, x = cH [H/Me] and Q is the heat of reaction. The enthalpy and entropy of the metal hydrides formation and hydrogen release determines the favourable temperature and pressures of the hydrogen storage materials. Most of the metal hydrides have higher thermodynamic stabilities which require the temperatures greater than 300°C at pressure of 1 bar. Some of the examples of metal hydrides are of alkaline earth metals, alkaline metals, rare earth metals, as well as transition metals of Sc (scandium)-, Ti (titanium)- and V (vanadium)-group (Dornheim 2011). The storage data for high and low temperature hydrides is given in Table 10.3.

10.4   Metal Hydride Properties

10.4.1   Metal Hydrides Available

The light weight metals such as Li (lithium), Be (beryllium), Na (sodium), Mg (magnesium), B (boron), and Al (aluminium) form a variety of metal hydrides which are majorly known for their light weight and number of hydrogen atom per metal atom (Bobet et al. 2000).

10.4.1.1 Mg Based Metal Hydride

Mg and Mg based alloys have shown high gravimetric hydrogen storage densities. Mg is the eight most frequent elements in earth which makes it relatively inexpensive. The Mg–H bond are highly stable with high enthalpy of hydride formation. Mg based hydrogen storage can be classified into three categories which are, Pure Mg, Mg-based alloys, Mg-based composites. In case of pure hydrogen the hydrogen storage capacity is extremely high with a reported gravimetric capacities of 7.6 wt% but the dissociation of compound will require higher temperatures and the reaction kinetics are very slow, it takes 50 h (50 h) for the complete formation of MgH_2 (magnesium hydride) at 350 °C and the enthalpy of desorption is $\Delta H = -74$ kJ/mol of H_2 which limits the use of pure Mg based hydrogen in practical applications. Moreover, the stability of MgH_2 made it to be useful in many suitable applications (Ouyang et al. 2020).

To improve the performance those pure Mg hydrides, some catalysts are added as additives such as transition metals or metal oxide elements. These additives are responsible for the change of surface properties, microstructures and grain growth with minimum affect to the storage capacity. To further improve the performance of MgH_2 some of the sample preparation methods such as smelting, diffusion, powder sintering, heat treatment and surface treatment methods can be adopted. Among them the most commonly used technique is reactive mechanical milling which will vary the microstructures of the metal to modify their properties. The main advantages of the method are the generation of reactive and fresh surfaces, the ease of formation of multiphase nano composites and creation of micro strains in crustal lattice. Several parameters of milling can be varied considering the end product of ball milling, such as milling speed, ball to powder weight ratio, milling time, milling atmosphere and temperature of the milling (Zhao and Zhang 2014).

If we change the entropy and enthalpy and of a hydrogenation reaction in an effective way to decrease the desorption temperature of MgH_2 systems. To modify those properties some of the methods such as alloying, nano structuring, changing the reaction paths and metastable phase formation are identified (Song et al. 2020).

Alloying

In case of alloying the Mg based alloys are usually made with a hydrogen non forming element which forms a less stable hydride decreasing the hydrogen reaction enthalpy. Materials such as counter rare earth (eg: Ce (cerium), La (lanthanum)), non-transition metals (eg: Al (aluminium), In (indium)) and transition metals (eg: Ni (nickel), Co (cobalt), Fe (iron), Cu (copper), Ag (silver), Sc (scandium), Y (yttrium), etc., have been identified to form a suitable-alloys for performance improvement of Mg based hydrides (Cui et al. 1999). Based on the bond formation three-categorizations of Mg based alloys are found such as solid solution compounds, intermetallic compounds, and other compounds (Ouyang et al. 2020).

Intermetallic Compound

Some of the intermetallic compounds such as Mg_2NiH_4 (magnesium nickel hydride), Mg_2FeH_6 (magnesium iron hexahydride), Mg_2CoH_5 (dimagnesium cobalt pentahydrate) have shown potential change in thermodynamic and kinetic properties (Cracco and Perchergon-Guegon 1998). In those materials if we consider Mg_2NiH_4 compound, Mg_2Ni is a potential hydrogen storage material with gravimetric capacity of 3.6 wt%, Mg_2NiH_4 has of $\Delta H = -64.5$ kJ mol^{-1} H_2 which gives the desorption temperature of 523 k with plateau pressure of 3 bar at room temperature (Ouyang et al. 2020).

Similar to Mg–Ni system, the Mg_2Cu alloy can form from the Mg and Cu (Sun et al. 1999). When Mg_2Cu is applied with 30 MPa hydrogen pressure, it decomposes to $MgCu_2$ and MgH_2 according to the following reaction:

$$Mg_2Cu + H_2 \Rightarrow MgH_2 + MgCu_2 \qquad (10.7)$$

The hydride enthalpy of formation is of -73.5 kJ(mol^{-1}H$_2$), hydrogen storage capacity is of 2.6 wt% and equilibrium temperature for 1 bar of hydrogen pressure is reduced to about 513 K but unfortunately this reaction is irreversible (Ouyang et al. 2020). In case of Mg_2FeH_6 which is formed by the mechanical milling of Mg and Fe in presence of hydrogen has hydrogen formation enthalpy of 98 kJ (mol^{-1} H_2) (Liang et al. 1998). It has shown a volumetric hydrogen density of 150 kg m^{-3} and gravimetric capacity of 5.6 wt% the which is more than that of liquid hydrogen at 20.2 K and moderate pressure up to 20 bar (Raman et al. 2002). Similar to the Mg–Fe system, ball milling of Mg and Co in the presence of hydrogen led to formation of Mg_2CoH_5 material with gravimetric capacity of 4.5 wt% and ΔH of -82 kJ mol^{-1} H_2 and desorption temperature of 513 K at 1 bar pressure (Wang et al. 2006).

Mg Based Solid Solution

Formation of Mg based solid solution is another strategy for destabilization which applies a minor modulation to the composition and structure (Zhu et al. 1999). Cadmium exhibits unlimited solubility in Mg. Mg^{-1} in the presence of Cd alloy can absorb 5 wt% hydrogen at 673 K in 24 h (Zhang et al. 2019). Mg_3Cd alloy using high energy milling have exhibited a gravimetric capacity of 2.8 wt% at 573 k in 120 s and ΔH is -65.5 kJ mol^{-1} (Skripnyuk and Rabkin 2012).

In the same way Mg–In system has high solubility of 10 at% indium at wide range of temperatures. The $Mg_{0.95}In_{0.05}$ solid solution can react with hydrogen reversibly at 573 k according to the following reaction (Cui et al. 2018):

$$Mg_{95}In_5 + 0.9H_{22} \Leftrightarrow 0.9MgH_2 + 0.05MgIn \qquad (10.8)$$
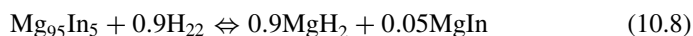
$Mg_{0.95}In_{0.05}$ have shown a gravimetric capacity of 5.3 wt% with the poor kinetics of desorption/absorption reaction. Therefore, ternary alloys such as Mg (In, Al), Mg (In, Cd) and Mg (In, Y) were investigated (Wang et al. 2014; Zhong et al. 2011).

In case of $Mg_{90}In_5Cd_5$ the reaction with H_2 goes as follows:

$$Mg_{90}In_5Cd_5 + 70\,H_2 \Leftrightarrow 70MgH_2 + 5MgIn + 5Mg_3Cd \qquad (10.9)$$
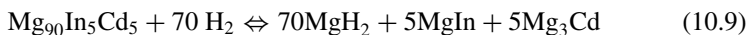
Here the dehydriding reaction enthalpy is found to be 86 kJ (mol^{-1} H$_2$). It has shown gravimetric capacity of 4.3 wt% (Xu et al. 2019). It also exhibited improved hydrogen kinetics and reduced hydrogenation activation energy of 61 kJ mol^{-1} but its dehydrogenation rate is slow because of long range diffusion of Cd and In and in MgH_2 (Lu et al. 2015).

Nano-structuring

In nano structuring the dimensionality of the architecture is the main feature for example: (i) zero dimensional (quantum dots, nanoparticles, and hollow spheres), (ii) one dimensional (nanorods, nanowires, nanofibers, and nanobelts) and (iii) three dimensional (frameworks, nanoflowers, and dendric structures) (Jepsen et al. 2017). Nanomaterials offer numerous advantages for hydrogen storage systems as the decrease in size of the material, its surface to volume ratios increases apparently. The atoms at the surface have dangling bonds which are extremely active and form strong bonds with surrounding molecules (Ouyang et al. 2020).

Nano particles or nano crystalline materials

Numerous methods can be used in the preparation of MgH_2 nano particles which includes melt spinning, ball milling and hybrid combustion. The surface energy density of magnesium is smaller than that of MgH_2, and some of the heat of formation can be stored as excess surface energy which reduces the heat release in the process of hydrogen release and hydride formation. Wagemans et al. (2005). The nanostructured uniform mixture of MgH_2–$0.1TiH_2$ powder has a cyclic hydrogen storage capacity 6 wt% and the ΔH_{des} is found to be 68 kJ (mol^{-1} H$_2$) (Zhang et al. 2019). Asano et al. concluded that embedding nano sized clusters of Mg in an immiscible metal matrix is found to beh the powerful strategy to destabilize MgH_2 which results in lower working temperatures (Asano et al. 2015). Carbon based nano materials has shown the potential in improving the gravimetric performance of MgH_2 (Zhang et al. 2017). Nanocomposite $(Mg-V)_{nano}$/G has shown a reversible gravimetric capacity of 6.03 wt% with enthalpy of formation of −68 kJ mol^{-1} of H_2 (Schneemann et al. 2018).

Nanowires and Nanofiber

Mg nanowires which have thin diameter has the advantage of easy activation for desorption/absorption of hydrogen. Changes in the thermodynamic properties are reported when the diameters of nanowires are thinner than 30 nm (Zaluska et al.

2001). Energy stability of Mg and MgH_2 nanowires were calculated using first principles density functional theory. The ΔH_{des} was calculated to be -20.64, 34.54, and $61.86 \, kJ(mol^{-1} \, H_2)$ for nano wires of A1_MgH_2($\varnothing 0.68$ nm), A2_MgH_2($\varnothing 0.85$ nm) and A3_MgH_2($\varnothing 1.24$ nm) (where $\varnothing$ indicates diameter of the nano wire) by which we can conclude that the decrease in diameter of the nano wire leads to energy instability in MgH_2 and Mg nanowires (Li et al. 2009).

Nanofilms

Thin films are largely applied in Mg materials. Mg nanostructured films were synthesized through various techniques which involve electron beam evaporation, Magnetron sputtering deposition, direct current and radio frequency, and plasma spatter. Thin film fabrication is an accurate method to control the nano structure, interfacial properties and composition of hydrogen storage materials (Schneemann et al. 2018).

10.4.1.2   Na Based Metal Hydrides

Sodium based metal hydrides can store the hydrogen in different forms. One method of storing the hydrogen is in the form of plastic-encapsulated NaH (sodium hydride) pellets. These pellets are cut into small slices and immersed in water where the NaH surface will react with water and produces sodium hydroxide and water. This method has shown a hydrogen storage density of 4.3 wt%. Sodium hydride and water reaction is strongly exothermic, so the reaction should take place in controlled environment.

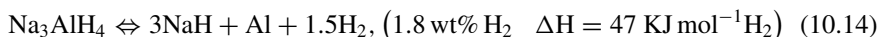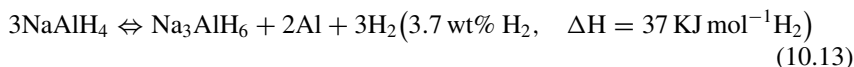$$NaH + H_2O \Rightarrow NaOH + H_2 \quad \Delta H = -35 \, kcal/mol \qquad (10.10)$$

The sodium hydroxide can again be converted into NaH by following certain steps such as (1) drying the sodium hydroxide, (2) raising the temperature of the system, (3) regenerating the hydroxide. The primary conversion involves reaction of sodium hydroxide with methane gas as shown in the below reaction:

$$NaOH + CH_4 \Rightarrow Na + CO + 2.5H_2 \qquad (10.11)$$

$$Na + 1/2H_2 \Rightarrow NaH \qquad (10.12)$$
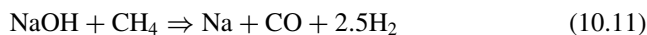
This method of hydrogen storage is not feasible for on-board applications as the conversion of NaOH to NaH is a high energy consuming process (DiPietro and Skolnik 2000). In all the alloys of sodium-based metal hydrides, sodium alanates are extensively investigated. One of the compounds which drawn attention is $NaAlH_4$. The atomic structure of sodium alanate consists of isolated $[AlH_4]^-$ tetrahedra structure where the sodium atoms are surrounded by the eight $[AlH_4]^-$ tetrahedra structures in a distorted square antiprismatic geometry. The reversible release and uptake of hydrogen of the selective additives dopped $NaAlH_4$ can take

place in two steps as described by the Eqs. (10.1 and 10.2).

$$3NaAlH_4 \Leftrightarrow Na_3AlH_6 + 2Al + 3H_2 \left(3.7\,wt\%\,H_2, \quad \Delta H = 37\,KJ\,mol^{-1}H_2\right)$$
$$\text{(10.13)}$$

$$Na_3AlH_4 \Leftrightarrow 3NaH + Al + 1.5H_2, \left(1.8\,wt\%\,H_2 \quad \Delta H = 47\,KJ\,mol^{-1}H_2\right) \quad \text{(10.14)}$$

The first reaction releases about 3.7 wt% of H_2 upon heating to a temperature of 190 °C and second reaction releases 1.8 wt% of H_2 upon heating to a temperature of 225 °C. The hydrogenation condition were considered to be severe as they have the operating temperature of 200–400 °C and pressures of 10–40 MPa. In-order to optimize the operating temperatures and pressures for practical applications, doping of $NaAlH_4$ with other suitable materials is thoroughly investigated (Li et al. 2013).

Doping of TiB_2 in $NaAlH_4$ after milling has shown a gravimetric capacity of 5.21 wt% at 190 °C (Li et al. 2012). Chen et al. (2009) stated that when $CeCl_3$ (cerium chloride) is doped with $NaAlH_4$ the activation energies for first and second dehydrogenation were calculated to be 80.76 and 97.27 kJ mol^{-1}. Bitter et al .(2006) investigated the carbon nanofiber-supported $NaAlH_4$ with different size ranges of particles such as 1–10 µm, 2–10 nm and 19–30 nm prepared by wet chemical synthesis. The results showed that the maximum desorption rate temperature (T_{max}) was found to be 70 °C for 2–10 nm $NaAlH_4$, 164 °C for 19–30 nm $NaAlH_4$ and 186 °C for 1–10 µm $NaAlH_4$. The dehydrogenation of Ti-doped $NaAlH_4$ composite has occurred at appreciable rates at a temperature of about 100 °C, which shows their potential to be used as on-board hydrogen storage system. After adding the $CeAl_2$, $NaAlH_4$ has shown rapid reaction kinetics with reload of 4.9 wt% hydrogen in 20 min and 70% of hydrogen can be released in just first 6 min (Fan et a 2011).

Another approach to enhance the kinetic performance is to decrease the $NaAlH_4$ particle size. The micro meter sized Al and NaH which are formed by agglomeration during hydrogenation/dehydrogenation reaction will be prevented by adding nano-sized sodium alanate. The hydrogenation/dehydrogenation rates were enhanced and hydrogenation/dehydrogenation temperatures were decreased. After impregnation, $NaAlH_4$ nano particles were amorphous, desorption temperature of hydrogen got reduced significantly and reaction kinetics improved (Li et al. 2013).

$NaAlH_4$ Doping Methods

$NaAlH_4$ doping methods

In metal infiltration, $NaAlH_4$ is loaded in a autoclave along with the inert scaffold material, where the hydrogen gas is pressurized to 150–200 bar and heated to a temperature of 170–200 °C (Bogdanović et al. 2000). Nielsen et al. (2011) reported that melt infiltrated $NaAlH_4$ into nano porous carbon aerogels could release hydrogen in the room temperature itself ($T_{onset} = 33$ °C) and at 125 °C hydrogen release rates reached a maximum value when functionalized with 3 wt % $TiCl_3$ catalyst.

Solvent mediated infiltration

In solvent mediated infiltration method, hydrogen storage material is dissolved in solvent to form a homogenous solution. The main advantage of this method is that the process can be performed under milder conditions when compared to melt infiltration. Sun et al. (2008) proposed a space-confined nano materials obtained by NaAlH$_4$confining into ordered mesoporous silica. The space-confined NaAlH$_4$have shown faster kinetics, lower dehydrogenation temperature, higher reversibility and higher loading of 20% was achieved (Li et al. 2013).

High energy ball milling

The main advantages of using high energy ball milling are increase in surface area, formation of nano/micro structures and lattice defects creation on the interior and surface of metal hydride. Beattie et al. studied the structural difference between un-milled and milled NaAlH$_4$ and observed that milled NaAlH$_4$ performed better than the un-milled NaAlH$_4$ as a reversible hydrogen storage material (Ashby et al. 1963).
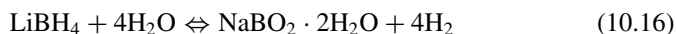
10.4.1.3 Boron Based Metal Hydrides

Boron based hydrogen storage materials which are generally represented as boranes and borohydrides are extensively investigated for potential hydrogen storage capability.

Boron based metal hydrides chemically store $4H^{\delta-}$ in the boron-hydride bonds. The main challenge involved is to recover 100% $H^{\delta-}$ in the form of H_2 molecule in mild conditions. The dehydrogenation can be carried out in two ways. The first one is hydrolysis of BBMs. In the presence of water, one $H^{\delta-}$ of BBM will react with one $H^{\delta+}$ of the H_2O molecule which liberates the H_2 molecule. The second method is thermolysis which consists of (i) intermolecular reaction and (ii) intramolecular reaction for the hydrogen release (Moussa et al. 2013).

Boron Based Hydrides for Hydrolysis

From all the borohydrides available so far LiBH$_4$, NaBH$_4$ and KBH$_4$ are considered under hydrolysis process.

$$NaBH_4 + 4H_2O \Leftrightarrow NaBO_2 \cdot 2H_2O + 4H_2 \tag{10.15}$$

$$LiBH_4 + 4H_2O \Leftrightarrow NaBO_2 \cdot 2H_2O + 4H_2 \tag{10.16}$$

$$KBH_4 + 4H_2O \Leftrightarrow KBO_2 \cdot 2H_2 \tag{10.17}$$

Among them only $NaBH_4$ is investigated excessively because of problems associated with other two such as hygroscopicity and spontaneous H_2 evolution, low gravimetric hydrogen storage capacity, slow H_2 release kinetics and clogging (Zhu et al. 2006). $NaBH_4$ also faces certain issues relating to low net hydrogen storage capacity, catalyst durability and positioning. The gravimetric hydrogen storage capacity of $NaBH_4$–H_2O is 7.3 wt% when there are 4 mol of H_2O for one mole of $NaBH_4$ for the hydrolysis reaction. The net gravimetric hydrogen storage capacity reported is 6–7 wt% in ambient conditions. The studies on $NaBH_4$ were more focused on prototyping, design of reactor, scalability, and coupling with reactor prototype. $NaBH_4$ was found to have more potential as a hydrogen carrier for mobile and portable applications (Moussa et al. 2013).

Same as $NaBH_4$, NH_3BH_3, hydrolysis in the presence of suitable catalyst the absolute net gravimetric capacity of the couple NH_3BH_3–$2H_2O$ is found to be 15 wt%, but it decreases to 9 wt% due to $3H^{\delta+}$ of the NH_3 moiety cannot be recovered. Furthermore, due to the by-products the storage capacity again decreases to 7.8 wt%. Liberation of ammonia is the main problem associated with using NH_3BH_3 in hydrolysis (Andrieux et al. 2012; Marrero-Alfonso et al. 2007; Moussa et al. 2013). If N_2H_4 moiety of the $N_2H_4BH_3$ can be dehydrogenated in the mild conditions in the presence of selective catalyst then $N_2H_4BH_3$–$3H_2O$ has shown the gravimetric capacity of 10 wt%. In the presence of bimetallic nano-catalyst ($Ni_{0.89}Pt_{0.11}$) in excess water and 50 °C, the dehydrogenation of $N_2H_4BH_3$ resulted in 5.8 mol $H_2 + N_2$ per mole which means 9.7 wt% of H_2 release is found. The main problem associated with all the products of boron-based material hydrolysis is their regenerability (Moussa et al. 2013).

Boron Based Hydrides for Thermolysis

$LiBH_4$ is considered as the most important hydride for thermolysis process. The main problem with the $NaBH_4$ is its thermal stability due to which it dehydrogenates at 530 °C (Züttel et al. 2003). The gravimetric hydrogen storage capacity of $LiBH_4$ was reported to be 18.5 wt% by thermolysis (Moussa et al. 2013). Pristine $LiBH_4$ melts and concomitantly decomposes over a temperature of 275 °C. The $LiBH_4$ dehydrogenation is partial

$$LiBH_4 \Rightarrow LiH + B + 3/2\ H_2 \qquad (10.18)$$
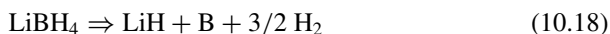
Therefore, the excess gravimetric heat storage capacity of $LiBH_4$ decreases to 13.9 wt%. The main advantage of using $LiBH_4$ lies in its possibility of reversibility. It was studied that the solid by products B and LiB can be hydrogenated to $LiBH_4$ at a temperature of 600 °C and under a H_2 pressure of 30 MPa (Orimo et al. 2005). To alter the dehydrogenation and re-hydrogenation conditions of the $LiBH_4$ to be milder, three strategies are identified. The first strategy is to destabilize the $LiBH_4$ by incorporating a metal or metalloid element, a hydride or an amide. The second strategy is addition of catalysts such as metal oxides and metal chlorides. For instance, it was reported

that by adding 25 wt% TiO_2 the dehydrogenation temperature decreased to 100 °C and H_2 release rate of 3 wt% within a temperature range of 100–300 °C (Au et al. 2008). The third strategy was to decrease the particle size of the $LiBH_4$ to down to nanoscale by nanoconfinement scaffolds. For instance, $LiBH_4$ impregnated into micro-cellular carbon foam dehydrogenates from a temperature of 200 °C so that 4 wt% of H_2 are released at a temperature of 300 °C (Brun et al. 2010).

Magnesium borohydrides $Mg(BH_4)_2$ is found to be the most suitable compound for hydrogen storage. It will liberate all of its hydrogen which is 14.9 wt% when heated upto 600 °C (Matsunaga et al. 2008). Calcium borohydride $(Ca(BH_4)_2)$ is the another much investigated borohydride which contains hydrogen capacity of 11.6 wt%. It partly dehydrogenates 9 wt% of H_2 under heating which follows a two-step reaction starts at 360 °C and it finishes at 500 °C (Miwa et al. 2006). Ammoni-aborane is also an attractive solution for thermolysis hydrogen storage material as it stores 19.5 wt% H and offers $3H^{\delta+}$ and $3H^{\delta-}$ can also combine together intermolec-ular and intermolecular interactions to give $3H_2$. At a temperature below −40 °C, NH_3BH_3 exists in a compound form which is richer in hydrogen; the hydrogen form is represented as NH_4BH_4 which is a densest material with gravimetric capacity of 24.3 wt% (Parry et al. 1958).

10.4.1.4   Aluminium Based Hydrogen Storage

Aluminium hydride is considered to be the promising candidate as a hydrogen storage material due to its high energy storage density. Aluminium hydride (AlH_3) exists as metastable, crystalline compound at the room temperature. It has the volumetric hydrogen density of 148 g H_2/L and the gravimetric hydrogen density that exceeds 10 wt%. It exhibits a heat of reaction of 7 kJ/mol of H_2 and at temperatures below 100 °C it has rapid hydrogen evolution rates (Graetz et al. 2011).

α-AlH_3 decomposes to products Al and H_2 by an endothermic reaction:

$$\alpha - AlH_3 \Rightarrow Al + 3/2\,H_2 \qquad (10.19)$$
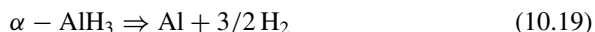
The experimentally determined enthalpy of formation ranges from −6.0 to −7.6 kJ/mol H_2 with entropy of formation of −129 J/k mol H_2 (Graetz et al. 2011). Compared to α-AlH_3 β and γ-AlH_3 structures are less stable. They undergo an exothermic transition to get converted to α at elevated temperatures greater than 100 °C.

Graetz and Reilly (2006) investigated the decomposition of α, β and γ-AlH_3 materials which are prepared form micro crystallization route. The transformation of less stable β and γ to α structure occurs very rapidly at temperatures above 100 °C.

Destabilization of aluminium hydride is extensively investigated for low tempera-ture fuel cell applications where rapid hydrogen evolution is required at temperatures lower than 100 °C. The thermal stability and the decomposition activation energy of the hydride mainly depend upon the material synthesis condition and its purity. It is

observed that alane is very sensitive towards light. Even for a short period exposure to the visible light the activation energy decreases by 15–20% when compared to non-irradiated fresh samples. Addition of transition metals and alkali hydrides has also shown the destabilization effect. Additions of transition metals have shown the pronounced effect on the decomposition kinetics when the synthesis of the AlH_3 is done by adding catalyst in the solution. In case of adding Ti the enhancement in the H_2 evolution rate can be seen at certain levels of few parts per million when Ti material was introduced in solution (Parry et al. 1958).

In-spite of all the advantages of the aluminium hydrides, it has a major limitation with bad reversibility of desorption which has hindered its practical applications in hydrogen storage carrier. To make the aluminium hydride a potential material for hydrogen storage, alantes are considered as a promising material. Among them $LiAlH_4$ and $NaAlH_4$ have attracted extensive attention. $LiAlH_4$ have shown the gravimetric capacities of 10.5 wt% H_2 with limitations of poor reversibility and unsatisfactory kinetics of desorption. Besides, $NaAlH_4$ have shown a theoretical gravimetric capacity of 7.4 wt % with excellent reversibility (Kumar et al. 2008).

Research is carried out on nano confinement of $LiAlH_4$ and $NaAlH_4$ to increase their potential in practical applications. Jiao et al. synthesized the $LiAlH_4$ with NiCo-doped nanoalloy which is encapsulated in graphene layers (NiCo@G). He found that the dehydrogenation temperature of $LiAlH_4$-NiCo@G is reduced to 36 °C. In the molecule 5% Fe_2O_3–$LiAlH_4$ the dehydrogenation temperature was found to be reduced to 70 °C and in the first two dehydrogenation process about 7.4 wt% of H_2 can be released (Jiao et al. 2016). Li et al. observed that the 2 mol% of $CoFe_2O_4$ doped $LiAlH_4$ shows good catalytic effect. The first dehydrogenation step occurs at 65 °C and the second occurs at 130 °C. This system can release 7.2 wt% of hydrogen (Li et al. 2014). Some of the hydrogen storage properties of nano confined metal hydrides is shown in Table 10.4.

10.4.2 Equilibrium Pressure for Metal Hydrides

The equilibrium pressure of the metal hydrides at different temperatures plays very important role in designing the hydrogen storage systems. For the calculation of equilibrium pressure, the reaction entropy and enthalpy for the metal hydride is required. The equilibrium pressure based on the entropy and enthalpy and of the reaction is given by:

$$P_{H_2}[\text{atm}] = \exp[(\Delta H - T\Delta S)/RT] \qquad (10.20)$$

where, $P_{H_2}[\text{atm}]$ is the equilibrium pressure, T is the temperature, ΔS is the change in entropy and ΔH is the change in enthalpy.

Based on the above equation the equilibrium pressure required can be calculated by taking the entropy and enthalpy of the various metal hydrides can be calculated. In

Table 10.4 Hydrogen storage properties of nano confined metal hydrides (Schneemann et al. 2018)

Hydride	Porous host	D_{avg} (nm)	V_{tot} ($cm^3 g^{-1}$)	Infiltration method	Solvent or atmosphere	H_2 wt%	References
Mg–H_2	RF-aerogel		1.27	$MgBu_2$	$170 - 200\,°C$, $50 - 78$ bar H_2, Ar, heptane	0.62	Nielsen et al. (2009)
Mg–H_2	RF-aerogel	27.1	1.32	$MgBu_2$	$150\,°C$, 150 bar H_2	1.8	Huen et al. (2017)
Mg–H_2	Ni-doped hollow carbon	3.4	1.53	$MgBu_2$	$NH_2NH_2 \cdot H_2O$	6.63	Shinde et al. (2017)
AlH_3	HSAG	2–3	0.66	Solvent impregnation	Et_2O	0.25	Wang et al. (2019)
$LiBH_4$	CMK-3	4.51	1.3	Grinding/melt infiltration	$310\,°C$, 60 bar H_2	3.4	Gosalawit-Utke et al. (2013)
$LiBH_4$	Pyrolyzed aerogel	13	0.8	Melt infiltration	$280 - 300\,°C$, Ar	12.5	Gross et al. 2008)
$LiBH_4$	Activated carbon	1.75–3.2	0.87	Solvent impregnation	THF	9	Fang et al. (2008)
NaH	HSAG	2–3	0.66	Physical mixing	Ar	4.4	Li et al. (2016)
$NaBH_4$	HSAG	2–3	0.66	Metal infiltration	$520\,°C$, 5 bar H_2	7.9	Adelhelm et al. (2010)

the equation R is universal gas constant which is taken as 8.314 ($J\,K^{-1}\,mol^{-1}$) (Brooks et al. 2020). Van't Hoff's lines for various metal hydrides is shown in Fig. 10.1.

10.4.3 Thermal Modelling of Metal Hydrides

The thermal properties such as specific heat capacity and thermal conductivity are usually required for analysing the thermodynamics of metal hydride.

Assumptions of the model:

(1)   The ideal gas equation of state is appropriate for the hydrogen gas.
(2)   Heat transfer through the form of radiation is negligible.
(3)   The viscous dissipation and compression work is negligible.
(4)   Gases and solids have same temperature.
(5)   Pressure variations affect is neglected.
(6)   Equilibrium pressure dependence on the hydrogen concentration is neglected.
(7)   The dispersion terms and tortuosity can be modelled as diffusion fluxes.

Fig. 10.1 Van't Hoff's lines
for various metal hydrides
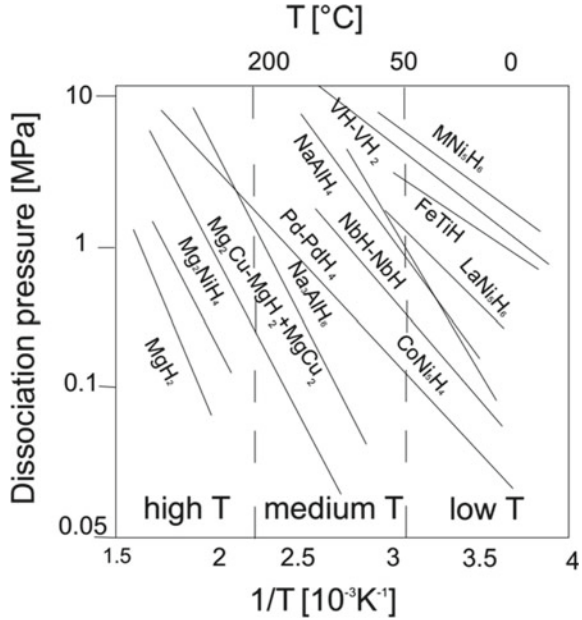
10.4.3.1 Thermodynamic Equations

As the dehydration and hydration of the metal hydrides is based on the temperature,
it is required to analyse the temperature profile.

The general equation for the variation of the internal energy for a porous metal
hydride is given by

$$\frac{\partial \rho U}{\partial t} = -(\overrightarrow{\nabla} \cdot \rho U \overrightarrow{v}) - (\overrightarrow{\nabla} \cdot \vec{q}) + Q - P(\overrightarrow{\nabla} \cdot \overrightarrow{v}) \qquad (10.21)$$

In the above equation U is the internal energy between two equilibrium states. $\vec{v}$ is
the fluid velocity. Heat added and removed from the system in the form of convection
or internal energy is given by Q, ρ is the density and heat transferred by convection
is given by q. The term $P(\overrightarrow{\nabla} \cdot \overrightarrow{v})$ represents the compression work which is usually
neglected.

Here, U can be re-written as

$$U = H - P/\rho \qquad (10.22)$$

Substituting the Eq. (10.3) in Eq. (10.2) and using the substantial derivatives gives

$$\rho \frac{DH}{Dt} = -(\vec{\nabla} \cdot \vec{q}) + Q + \frac{DP}{Dt}. \qquad (10.23)$$

Enthalpy can be expressed as the function of pressure and temperature

$$\frac{DH}{Dt} = C_p \frac{DT}{Dt} + \left(\frac{1}{\rho} + \frac{T}{\rho^2} \frac{\partial \rho}{\partial T} \right) \frac{DP}{Dt} \tag{10.24}$$

In the above equation C_p is the specific heat capacity.

Substituting the Eq. (10.5) in Eq. (10.4) we get

$$\rho C_p \left(\frac{\partial T}{\partial t} + \vec{v} \cdot \nabla T \right) = \lambda \cdot \nabla^2 + Q - \frac{\partial \ln \rho}{\partial \ln T} \left(\frac{\partial P}{\partial t} + \vec{v} \cdot \nabla P \right) \tag{10.25}$$

where for an ideal gas $\frac{\partial \ln \rho}{\partial \ln T} = -1$.

Energy balance equations for the solid and gas combined can be expressed as

$$\left(\rho C_p \right)_e \frac{\partial T}{\partial t} = \lambda_e \nabla^2 T - \rho_g C_{pg} \vec{v} \cdot \nabla T + m \left(\Delta H + T \left(C_{pg} - C_{ps} \right) \right) \tag{10.26}$$

$$\left(\rho C_p \right)_e = \varepsilon \rho_g^g C_{pg} + (1 - \varepsilon) \rho_s^s C_{ps} \tag{10.27}$$

where, m is the mass of the metal hydride, ε is the porosity of the metal hydride bed. The term g designates the gas phase and s designates the solid phase. λ_e is the effective thermal conductivity of the metal hydride bed, effective thermal conductivity mainly depends on the thermal conductivity of the solid and gas and also on the structural properties of the porous media.

$$\lambda_e = \varepsilon \lambda_g + (1 - \varepsilon) \lambda_s \tag{10.28}$$

where, λ_g is the thermal conductivity of hydrogen gas and λ_s is the thermal conductivity of metal powder.

10.4.3.2   Reaction Kinetics of Metal Hydrides

Rate law of reaction hydrogen uptake and discharge is defined by m. it is the relationship between the reaction rate and species concentration. The value of the rate of reaction is given by the equation as follows

$$m_a = C_a \exp \left(-\frac{E_a}{R_g T} \right) \ln \left(\frac{P_g^g}{P_{eqa}} \right) [\rho_{ss} - \rho_s] \tag{10.29}$$

$$m_d = C_d \exp \left(-\frac{E_a}{R_g T} \right) \left[\frac{P_g^g - P_{eqd}}{P_{eqd}} \right] \tag{10.30}$$

where, ρ_{ss} is the metal hydride density at the end of the absorption. ρ_s is the density of the metal powder without hydrogen. The reaction constants follow Arrhenius

equation for both desorption and absorption process. P_{eq} is the equilibrium pressure of the metal hydride system. The difference between the pressure of the system and the equilibrium pressure is the driving force for the sorption process.

The Van't Hoff equation will give the relation for calculating the equilibrium pressure and temperature of the hydride.

$$\ln P_{\text{eq}} = \frac{\Delta H}{R_{\text{gT}}} - \frac{\Delta S}{R_{\text{g}}} \tag{10.31}$$

This is same as the equation mentioned above to calculate pressure according to the enthalpy and entropy (Mohammadshahi et al. 2016).

10.5 Requirements of Metal Hydrides for On-Board Applications

The metal hydrides are selected for automobile applications only when then cross the DOE targets. The DOE has set targets on properties such as system system volumetric capacity, gravimetric capacity, durability/operability, storage system cost, charging/discharging rates, fuel quality, environmental, health and safety.

10.5.1 Achieving the Required Pressure

To achieve the proper performance of metal hydrides pressure variations should be achieved inside the storage tank. The dehydrogenation and hydrogenation rates depend on pressure inside the storage tank. As discussed above different metal hydrides require different pressure conditions according to the temperature of operation. The release rate of hydrogen from the metal hydride will also depend on the pressure. Increase in hydrogenation rates of the metal hydrides is observed by creating a vacuum pressure to suck out the air particles from the storage tank.

In-order to achieve the required pressure metal hydride compressors can be used. Metal hydride thermal sorption compression is a reliable efficient method which allows conversion of heat energy into compressed hydrogen gas. For improving the hydrogen storage characteristics, several features are required to be optimized such as pressure plateaus synchronization for multi stage compressors, slope of the isotherm reduction and hysteresis, increase in the life time and cyclic stability and the system design which is associated with the volume expansion of the metal matrix during the hydrogenation (Kumar et al. 2018).

Optimizing the metal hydride compressors mainly depends upon finding a compromise between contradicting factors. The first group A type of factor should assure matching available temperatures and specified pressures, maximum reversible
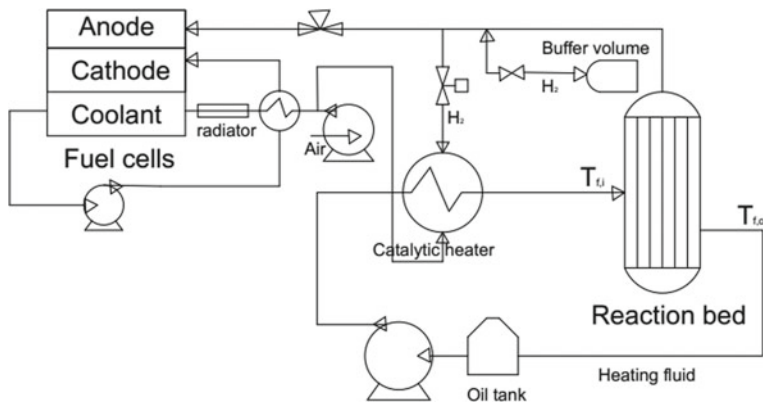
Fig. 10.2 System flow chart for metal hydride storage system coupled with fuel cells

sorption capacity, heat capacity and minimal dilution. The second group B and third group C factors are mainly related to design optimization of metal hydrides compressor, operating conditions and its manufacturing technologies (Lototskyy et al. 2014). HYSTORE technologies Ltd. (with the assistance of other research partners) has developed a small-scale metal hydride compressor demonstrator. The demonstrator operated in 6 stages; each stage deals with the specialized metal hydrides. It is found to be raising the hydrogen gas pressure from <5 bar to more than 200 bar by using water as heat exchanger fluid. The system achieves a stable hydrogen flow of about 3 Nm^3/h (Stamatakis et al. 2018). The system flow chart for metal hydride storage system coupled to fuel cells is as shown in Fig. 10.2.

10.5.2 Achieving the Required Heat Transfer

The heat transfer in metal hydride storage systems is the major parameter which controls the storage process. The main factors governing the heat transfer are enhancement of thermal conductivity of the bed by use of metal forms or ENG compacts, reduction in the reactor bed radius, increase in heat transfer area and increase in heat transfer mass flow rate and velocity.

Balzarotti et al. (2020) investigated a method of using pellets of Cu coating and Ni foam for improvement in thermal conductivity. The results showed that the Ni foam is an cost effective method of improving the thermal conductivity. Sanchez et al. investigated the effect of graphite compacts and foam to improve the thermal conductivity and found that the method has shown improvement in heat transfer but the major disadvantage is the compacts has shown to be deteriorated over prolonged usage (Sánchez et al. 2003). Botzung et al. (2008) investigated the effect of Al fins and foam in improving the thermal conductivity and found the significant improvement in thermal conductivity (Wang et al. 2019). Yang et al. (2008), studied the
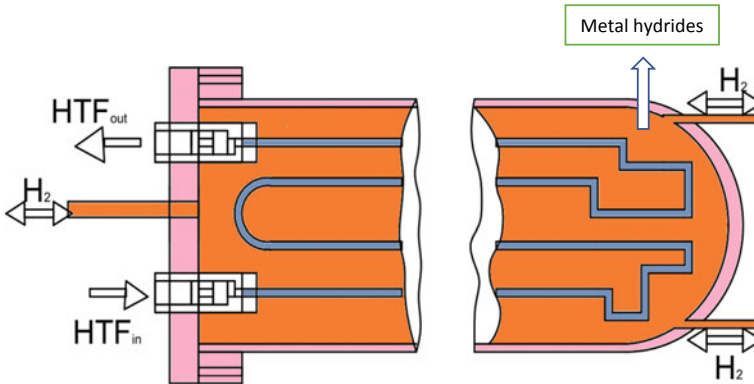
Fig. 10.3 Reactor bed design for the metal hydrides with heat transfer fluid

disc reactor, tubular reactor and annulus disc reactor for improvement in thermal conductivity and heat transfer. The system performance was found to be improved in heat transfer-controlled reaction rate and mass-transfer controlled reaction rate. Ranong et al. (2009) investigated the multiple metal hydride tank and cooling tube in single tank to improve the heat transfer area. It was found that the both designs have shown comparable performances and coiled tubes have shown better gravimetric capacity. Krokos et al. (2009), investigated the geometric optimization and heat transfer velocity optimization for improvement in heat transfer area. The system is observed to capable of an on-board storage for upto 25 km. Dhaou et al. (2010), investigated the double spiral heat exchanger with or without fins and optimized the pitch and fin diameter. The heat exchange performance was increased by 70%.

Chung et al. (2013) investigated the effect of heat pipes with fins which is considered as non-convectional method. It is observed that there is 50% improvement because of the use of heat pipes. The system was not found to be effective for large scale systems. Garrier et al. (2013), investigated the metal hydride compact and phase change material jackets. He found that the PCM system is found to be effective for large scale systems. Mellouli et al. (2016, 2017) investigated the PCM jackets, central tube embedded units with spherical, cylindrical and hexagonal geometries. It is observed that the cylindrical design performs better than the rest of the PCM geometric reactors. Design for the reactor bed with metal hydrides is shown in Fig. 10.3. In the figure HTF$_{in}$ indicates heat transfer fluid inlet and HTF$_{out}$ indicates heat transfer fluid out.

10.5.3 Mass and Volume Considerations

The mass and volume are the major considerations which limited the use of metal hydrides as on-board hydrogen storage systems. Research is directed towards the

improvement in volumetric and gravimetric storage densities of the metal hydrides. Many methods such as alloying, nanoconfinement and ball milling are used to improve those parameters. Various techniques and their effect on different metal hydrides are reported in the previous sections.

Apart from the weight of the metal hydrides, the mass and volume of the storage tank also contributes to the major increase mass and volume in storage systems. The material selected for the tank must be of lower density. The thermal conductivity and heat capacity of the storage tank should also be considered. So the material selected for storage tank must be a compromise between the thermal properties and the density considerations. Along with the thermal properties the tank material properties such as corrosion resistance, mechanical strength and should not react with the chemical for the reaction to take place. Based on all these parameters the material should be selected to reduce the mass and volume requirements of the system. The gravimetric and volumetric capacities of the different types of metal hydrides are listed in the above sections.

10.5.4 Recyclability of Metal Hydrides for Many Cycles

The cyclic stability of the metal hydride is also a major parameter which governs the hydrogen storage capacity. Many researchers have tried to improve the cyclic stability of the metal hydrides. According to DOE targets the metal hydride should at least have cyclic stability up to 1500 cycles. Metal hydride composites were prepared which consists of a hydride consisting metal alloy and higher heat conduction material such as expanded natural graphite. The composite has shown a cyclic stability up to 1000 cycles at a constant temperature. The thermal conductivity was found to be decreased at the initial stages but later became constant (Nautiyal et al. 2015). It also showed the higher mechanical integrity. Some metal hydrides are identified as the relevant materials for practical applications. The metal hydrides include the types AB_5 alloys, AB_2 alloys and Mg (Ni). It was observed that the reversible storage capacity of AB_5 alloy decayed during the longer cycles. Even though the material loses its stability, the original stability can be restored by heating the material at 400–500 °C in vacuum conditions (Sakintuna et al. 2007).

Requirements of metal hydrides for on-board applications

Based on the above critical parameters, hydrogen storage systems which are mainly intended for automobile applications are tested and analysed by Giovanni Capurso (Capurso et al. 2018). In the research a metal hydride hydrogen storage tank with 10 cylinders containing 9.5 kg of hydride and the total mass of the system which includes frame, air circulating system, heat exchangers reached to 25 kg. After conducting the required tests simulating the vehicular applications, it was found that hydrogen release in an hour is more than 0.6 m^3 at a flow rate of 25 NL min^{-1}. The gravimetric capacity was found to 1.80 w% of H_2 with H_2 release of 1.65 wt% at the pressure above the fuel cell requirements. In absolute terms, the hydrogen usable is found to

be 155 g but the hydrogen stored was found to be in 170 g. The volumetric hydrogen storage capacity was resulted to be 115 g dm^{-3}.

The hydrogen quantity combined with the mass and the dimensions of the storage system yields H$_2$ system gravimetric capacity of 0.65 wt% and a system volumetric capacity was found to be 6.2 g dm^{-3}. The system is found to be accumulating the energy of more than 22 MJ (6.1 kWh) with a density of 0.88 MJ kg^{-1}. The properties of the hydrogen storage tank were reported to be compared with the specific energies of li-ion batteries, alkaline and lead acid batteries. However, the power density depends on the heat exchanger effectiveness (Du et al. 2019).

HySA systems in collaboration with TF design built a prototype of air heated/cooled cassette-type metal hydride tank which is used for light electric vehicles. The hydrogen storage material used in the tank is multicomponent AB$_2$ type hydrogen storage alloy. The material has shown a reversible hydrogen storage capacity of 170 NL H$_2$/kg (1.5 wt% H; T = 20 °C and P(H$_2$) = 40.1 bar) (Davids et al. 2019).

Mori et al. (2005) developed and tested a new type of high-pressure metal hydride tank for fuel cell vehicles with the collaboration of Toyota motors corporation. The tank is integrated with heat exchanger module and high-pressure cylindrical vessels. With a tank volume of 180 L the hydrogen storage capacity of 7.3 kg is achieved. In addition, the hydrogen is released at 243 K due to the hydrogen desorption alloy with a high dissociation pressure. The cursing range of over 700 km is achieved (Gupta el al. 2018).

10.6 Conclusion

Metal hydrides can be considered as the safest and compact alternative source for hydrogen storage. Over the past decade there was tremendous research going on for optimization of metal hydrides for on-board system requirement.

The present article reviews about the metal hydrides which have a potential to be used as hydrogen storage material. The metal hydrides should possess properties such as high hydrogen storage density, high gravimetric capacity, high cyclability, lower energy loss, light weight, low volumetric density etc. hydrogen should be stored in metal hydrides at moderate temperature and pressure. The research on metal hydrides is mainly focussed on improving its adsorption/desorption properties based on their hydrogen storage capacity, kinetics and thermal properties. Various methods were found to improve their performance. Based on the material properties different techniques are used on different materials. Some of the methods used were highlighted in the present article.

Among all the materials, Mg based metal hydrides are found to be the promising candidates for the hydrogen storage with a gravimetric capacity of 7.6 wt% with high hydrogen desorption capacity temperature of about 300 °C. Efforts are carried out to reduce the desorption temperature and improve the kinetics of the hydride by using appropriate production method, catalysts and nano structuring.

After Mg, the sodium-based hydrides were also identified as the promising candidates for the hydrogen storage with a gravimetric capacity of 4.5 wt% but the reversibility of the hydride posted a major problem. Various doping methods were identified to improve the reversibility and the hydrogen loading capacity of the sodium-based metal hydrides.

The equation required to calculate the equilibrium pressure at various temperatures based on the enthalpy and entropy of the metal hydride chemical reaction is represented in this article. Equations related to the modelling of hydrogen flow and heat transfer analysis based on the heat exchange system and the tank design were also represented in the present work.

The major requirements for the on-board storage system such as methods to achieve the required pressure and temperature for the metal hydride were highlighted. The mass and volume requirements of the metal hydride based on-board storage systems were discussed.

The feasibility of the metal hydrides hydrogen storage tank for the vehicular applications based on the parameters like gravimetric capacity, volumetric capacity, energy density were reported.

References

Adelhelm P, Gao J, Verkuijlen MH, Rongeat C, Herrich M, van Bentum PJM, Gutfleisch O, Kentgens AP, de Jong KP, de Jongh PE (2010) Comprehensive study of melt infiltration for the synthesis of NaAlH4/C nanocomposites. Chem Mater 22(7):2233–2238

Andrieux J, Laversenne L, Krol O, Chiriac R, Bouajila Z, Tenu R, Counioux JJ, Goutaudier C (2012) Revision of the NaBO$_2$–H$_2$O phase diagram for optimized yield in the H$_2$ generation through NaBH$_4$ hydrolysis. Int J Hydrogen Energy 37(7):5798–5810

Asano K, Westerwaal RJ, Anastasopol A, Mooij LP, Boelsma C, Ngene P, Schreuders H, Eijt SW, Dam B (2015) Destabilization of Mg hydride by self-organized nanoclusters in the immiscible Mg–Ti system. J Phys Chem C 119(22):12157–12164

Ashby EC, Brendel GJ, Redman HE (1963) Direct synthesis of complex metal hydrides. Inorg Chem 2(3):499–504

Au M, Spencer W, Jurgensen A, Zeigler C (2008) Hydrogen storage properties of modified lithium borohydrides. J Alloy Compd 462(1–2):303–309

Baldé CP, Hereijgers BP, Bitter JH, de Jong KP (2006) Facilitated hydrogen storage in NaAlH$_4$ supported on carbon nanofibers. Angew Chem 118(21):3581–3583

Balzarotti R, Ambrosetti M, Beretta A, Groppi G, Tronconi E (2020) Investigation of packed conductive foams as a novel reactor configuration for methane steam reforming. Chem Eng J 391:123494

Bobet JL, Akiba E, Nakamura Y, Darriet B (2000) Study of Mg-M (M=Co, Ni and Fe) mixture elaborated by reactive mechanical alloying—Hydrogen sorption properties. Int J Hydrogen Energy 25(10):987–996

Bogdanović B, Brand RA, Marjanović A, Schwickardi M, Tölle J (2000) Metal-doped sodium aluminium hydrides as potential new hydrogen storage materials. J Alloy Compd 302(1–2):36–58

Botzung M, Chaudourne S, Gillia O, Perret C, Latroche M, Percheron-Guegan A, Marty P (2008) Simulation and experimental validation of a hydrogen storage tank with metal hydrides. Int J Hydrogen Energy 33(1):98–104

Brooks KP, Sprik SJ, Tamburello DA, Thornton MJ (2020) Design tool for estimating metal hydride storage system characteristics for light-duty hydrogen fuel cell vehicles. Int J Hydrogen Energy 45(46):24917–24927

Brun N, Janot R, Sanchez C, Deleuze H, Gervais C, Morcrette M, Backov R (2010) Preparation of LiBH 4@ carbon micro–macrocellular foams: tuning hydrogen release through varying microporosity. Energy Environ Sci 3(6):824–830

Buchner H (1978) The hydrogen/hydride energy concept. Int J Hydrogen Energy 3(4):385–406

Capurso G, Schiavo B, Jepsen J, Lozano GA, Metz O, Klassen T, Dornheim M (2018) Metal hydride-based hydrogen storage tank coupled with an urban concept fuel cell vehicle: off board tests. Adv Sustain Syst 2(6):1800004

Chung CA, Yang SW, Yang CY, Hsu CW, Chiu PY (2013) Experimental study on the hydrogen charge and discharge rates of metal hydride tanks using heat pipes to enhance heat transfer. Appl Energy 103:581–587

Cracco D, Percheron-Guegan A (1998) Morphology and hydrogen absorption properties of an AB2 type alloy ball milled with Mg_2Ni. J Alloy Compd 268(1–2):248–255

Cui N, He P, Luo JL (1999) Magnesium-based hydrogen storage materials modified by mechanical alloying. Acta Mater 47(14):3737–3743

Cui J, Jonuzaj S, Adjiman CS (2018) A comprehensive approach for the design of solvent-based adhesive products using generalized disjunctive programming. In: Comput Aided Chem Eng, vol 44. Elsevier, pp 427–432

Davids MW, Lototskyy M, Malinowski M, van Schalkwyk D, Parsons A, Pasupathi S, Swanepoel D, van Niekerk T (2019) Metal hydride hydrogen storage tank for light fuel cell vehicle. Int J Hydrogen Energy 44(55):29263–29272

Dehouche Z, Djaozandry R, Goyette J, Bose TK (1999) Evaluation techniques of cycling effect on thermodynamic and crystal structure properties of Mg_2Ni alloy. J Alloy Compd 288(1–2):269–276

Dhaou H, Souahlia A, Mellouli S, Askri F, Jemni A, Nasrallah SB (2010) Experimental study of a metal hydride vessel based on a finned spiral heat exchanger. Int J Hydrogen Energy 35(4):1674–1680

DiPietro, J.P. and Skolnik, E.G., 2000. Sodium hydride-based hydrogen storage system. In *Proceedings of the 2000 DOE hydrogen program review NREL/CP-570–28890.*

Dornheim M (2011) Thermodynamics of metal hydrides: tailoring reaction enthalpies of hydrogen storage materials. IntechOpen

Du J, Lan Z, Zhang H, Lü S, Liu H, Guo J (2019) Catalytic enhanced hydrogen storage properties of Mg-based alloy by the addition of reduced graphene oxide supported V_2O_3 nanocomposite. J Alloy Compd 802:660–667

Fan X, Xiao X, Chen L, Yu K, Wu Z, Li S, Wang Q (2009) Active species of $CeAl_4$ in the $CeCl_3$-doped sodium aluminium hydride and its enhancement on reversible hydrogen storage performance. Chem Commun 44:6857–6859

Fan X, Xiao X, Chen L, Li S, Ge H, Wang Q (2011) Enhanced hydriding−dehydriding performance of $CeAl_2$-doped $NaAlH_4$ and the evolvement of Ce-containing species in the cycling. J Phys Chem C 115(5):2537–2543

Fang ZZ, Wang P, Rufford TE, Kang XD, Lu GQ, Cheng HM (2008) Kinetic-and thermodynamic-based improvements of lithium borohydride incorporated into activated carbon. Acta Mater 56(20):6257–6263

Garrier S, Delhomme B, De Rango P, Marty P, Fruchart D, Miraglia S (2013) A new MgH_2 tank concept using a phase-change material to store the heat of reaction. Int J Hydrogen Energy 38(23):9766–9771

Gizer G, Puszkiel J, Riglos MVC, Pistidda C, Ramallo-López JM, Mizrahi M, Santoru A, Gemming T, Tseng JC, Klassen T, Dornheim M (2020) Improved kinetic behaviour of $Mg(NH_2)_2–2LiH$ doped with nanostructured K-modified-$Li_xTi_yO_z$ for hydrogen storage. Sci Rep 10(1):1–12

Gosalawit-Utke R, Milanese C, Javadian P, Jepsen J, Laipple D, Karmi F, Puszkiel J, Jensen TR, Marini A, Klassen T, Dornheim M (2013) Nanoconfined 2LiBH4–MgH2–TiCl3 in carbon aerogel scaffold for reversible hydrogen storage. Int J Hydrogen Energy 38(8):3275–3282

Graetz J, Reilly JJ (2006) Thermodynamics of the α, β and γ polymorphs of AlH3. J Alloy Compd 424(1–2):262–265

Graetz J, Reilly JJ, Yartys VA, Maehlen JP, Bulychev BM, Antonov VE, Tarasov BP, Gabis IE (2011) Aluminum hydride as a hydrogen and energy storage material: past, present and future. J Alloy Compd 509:S517–S528

Gross AF, Vajo JJ, Van Atta SL, Olson GL (2008) Enhanced hydrogen storage kinetics of LiBH4 in nanoporous carbon scaffolds. J Phys Chem C 112(14):5651–5657

Gupta JG, De S, Gautam A, Dhar A, Pandey A (2018) Introduction to sustainable energy, transportation technologies, and policy. In: Sustainable energy and transportation. Springer, Singapore, pp 3–7

Huen P, Paskevicius M, Richter B, Ravnsbæk DB, Jensen TR (2017) Hydrogen storage stability of nanoconfined MgH2 upon cycling. Inorganics 5(3):57

Jepsen LH, Paskevicius M, Jensen TR (2017) Nanostructured and complex hydrides for hydrogen storage. Nanotechnol Energy Sustain, 415–432

Jiao C, Sun L, Xu F, Liu SS, Zhang J, Jiang X, Yang L (2016) NiCo nanoalloy encapsulated in graphene layers for improving hydrogen storage properties of LiAlH 4. Sci Rep 6(1):1–8

Kohno T, Tsuruta S, Kanda M (1996) The hydrogen storage properties of new Mg2Ni alloy. J Electrochem Soc 143(9):L198

Krokos CA, Nikolic D, Kikkinides ES, Georgiadis MC, Stubos AK (2009) Modeling and optimization of multi-tubular metal hydride beds for efficient hydrogen storage. Int J Hydrogen Energy 34(22):9128–9140

Kumar N (2019) Study of oxygenated ecofuel applications in CI engine, gas turbine, and jet engine. In: Azad A, Rasul M (eds) Advanced biofuels: applications, technologies and environmental sustainability, 1st edn. Elsevier, New York, pp 405–441

Kumar LH, Viswanathan B, Murthy SS (2008) Dehydriding behaviour of LiAlH4—the catalytic role of carbon nanofibres. Int J Hydrogen Energy 33(1):366–373

Kumar P, Srivastava KN, Dhar A (2018) Role of electric vehicles in future road transport. In: Sustainable energy and transportation. Springer, Singapore, pp 43–60

Li L, Peng B, Ji W, Chen J (2009) Studies on the hydrogen storage of magnesium nanowires by density functional theory. J Phys Chem C 113(7):3007–3013

Li L, Qiu F, Wang Y, Liu G, Yan C, An C, Xu Y, Wang Y, Song D, Jiao L, Yuan H (2012) Improved dehydrogenation performances of TiB2-doped sodium alanate. Mater Chem Phys 134(2–3):1197–1202

Li L, Xu C, Chen C, Wang Y, Jiao L, Yuan H (2013) Sodium alanate system for efficient hydrogen storage. Int J Hydrogen Energy 38(21):8798–8812

Li Z, Zhai F, Wan Q, Liu Z, Shan J, Li P, Volinsky AA, Qu X (2014) Enhanced hydrogen storage properties of LiAlH4 catalyzed by CoFe2O4 nanoparticles. RSC Adv 4(36):18989–18997

Li Y, Ding X, Zhang Q (2016) Self-printing on graphitic nanosheets with metal borohydride nanodots for hydrogen storage. Sci Rep 6(1):1–10

Liang G, Boily S, Huot J, Van Neste A, Schulz R (1998) Hydrogen absorption properties of a mechanically milled Mg–50 wt.% LaNi5 composite. J Alloys Compd 268(1–2):302–307

Lototskyy MV, Yartys VA, Pollet BG, Bowman RC Jr (2014) Metal hydride hydrogen compressors: a review. Int J Hydrogen Energy 39(11):5818–5851

Lu YS, Wang H, Ouyang LZ, Liu JW, Zhu M (2015) Reversible hydrogen storage and phase transformation with altered desorption pressure in Mg90In5Cd5 ternary alloy. J Alloy Compd 645:S103–S106

Lu C, Zou J, Zeng X, Ding W, Shao H (2019) Enhanced hydrogen sorption properties of core-shell like structured Mg@ NaBH4/MgB2 composite. J Alloys Compd 810:151763

Marrero-Alfonso EY, Gray JR, Davis TA, Matthews MA (2007) Minimizing water utilization in hydrolysis of sodium borohydride: the role of sodium metaborate hydrates. Int J Hydrogen Energy 32(18):4723–4730

Matsunaga T, Buchter F, Mauron P, Bielman M, Nakamori Y, Orimo S, Ohba N, Miwa K, Towata S, Züttel A (2008) Hydrogen storage properties of Mg[BH$_4$]$_2$. J Alloy Compd 459(1–2):583–588

Mellouli S, Abhilash E, Askri F, Nasrallah SB (2016) Integration of thermal energy storage unit in a metal hydride hydrogen storage tank. Appl Therm Eng 102:1185–1196

Mellouli S, Askri F, Abhilash E, Nasrallah SB (2017) Impact of using a heat transfer fluid pipe in a metal hydride-phase change material tank. Appl Therm Eng 113:554–565

Miwa K, Aoki M, Noritake T, Ohba N, Nakamori Y, Towata SI, Züttel A, Orimo SI (2006) Thermodynamical stability of calcium borohydride Ca (BH$_4$)$_2$. Phys Rev B 74(15):155122

Mohammadshahi SS, Gray EM, Webb CJ (2016) A review of mathematical modelling of metal-hydride systems for hydrogen storage applications. Int J Hydrogen Energy 41(5):3470–3484

Mori D, Haraikawa N, Kobayashi N, Kubo H, Toh K, Tsuzuki M, Shinozawa T, Matsunaga T (2005) High-pressure metal hydride tank for fuel cell vehicles. MRS Online Proceedings Library (OPL) 884

Moussa G, Moury R, Demirci UB, Şener T, Miele P (2013) Boron-based hydrides for chemical hydrogen storage. Int J Energy Res 37(8):825–842

Na Ranong C, Hoehne M, Franzen J, Hapke J, Fieg G, Dornheim M, Eigen N, Bellosta von Colbe JM, Metz O (2009) Concept, design and manufacture of a prototype hydrogen storage tank based on sodium alanate. Chem Eng Technol Ind Chem-Plant Equip-Process Eng-Biotechnol 32(8):1154–1163

Nautiyal H, Shree V, Khurana S, Kumar N, Varun (2015) Recycling potential of building materials: a review. In: Muthu SS (ed) Environmental footprints and eco-design of products and processes, 1st edn. Springer, New York, pp 31–50

Nielsen TK, Manickam K, Hirscher M, Besenbacher F, Jensen TR (2009) Confinement of MgH$_2$ nanoclusters within nanoporous aerogel scaffold materials. ACS Nano 3(11):3521–3528

Nielsen TK, Polanski M, Zasada D, Javadian P, Besenbacher F, Bystrzycki J, Skibsted J, Jensen TR (2011) Improved hydrogen storage kinetics of nanoconfined NaAlH$_4$ catalyzed with TiCl$_3$ nanoparticles. ACS Nano 5(5):4056–4064

Orimo SI, Nakamori Y, Kitahara G, Miwa K, Ohba N, Towata SI, Züttel A (2005) Dehydriding and rehydriding reactions of LiBH$_4$. J Alloy Compd 404:427–430

Orimo SI, Nakamori Y, Eliseo JR, Züttel A, Jensen CM (2007) Complex hydrides for hydrogen storage. Chem Rev 107(10):4111–4132

Ouyang L, Liu F, Wang H, Liu J, Yang XS, Sun L, Zhu M (2020) Magnesium-based hydrogen storage compounds: a review. J Alloys Compd 832:154865

Parry RW, Schultz DR, Girardot PR (1958) The preparation and properties of hexamminecobalt (III) borohydride, hexamminechromium (III) borohydride and ammonium borhydride1. J Am Chem Soc 80(1):1–3

Raman SS, Davidson DJ, Bobet JL, Srivastava ON (2002) Investigations on the synthesis, structural and microstructural characterizations of Mg-based K$_2$PtCl$_6$ type (Mg$_2$FeH$_6$) hydrogen storage material prepared by mechanical alloying. J Alloy Compd 333(1–2):282–290

Reilly JJ, Wiswall RH (1974) Formation and properties of iron titanium hydride. Inorg Chem 13(1):218–222

Sakintuna B, Lamari-Darkrim F, Hirscher M (2007) Metal hydride materials for solid hydrogen storage: a review. Int J Hydrogen Energy 32(9):1121–1140

Sánchez AR, Klein HP, Groll M (2003) Expanded graphite as heat transfer matrix in metal hydride beds. Int J Hydrogen Energy 28(5):515–527

Saxena V, Kumar N, Saxena V (2021) Combustion, performance and emissions of *Acacia concinna* biodiesel blends in a diesel engine with variable specific heat ratio. J Therm Anal Calorim. https://doi.org/10.1007/s10973-020-10483-7

Schneemann A, White JL, Kang S, Jeong S, Wan LF, Cho ES, Heo TW, Prendergast D, Urban JJ, Wood BC, Allendorf MD (2018) Nanostructured metal hydrides for hydrogen storage. Chem Rev 118(22):10775–10839

Shinde SS, Kim DH, Yu JY, Lee JH (2017) Self-assembled air-stable magnesium hydride embedded in 3-D activated carbon for reversible hydrogen storage. Nanoscale 9(21):7094–7103

Skripnyuk VM, Rabkin E (2012) Mg3Cd: A model alloy for studying the destabilization of magnesium hydride. Int J Hydrogen Energy 37(14):10724–10732

Song W, Dong H, Zhang G, Liu J, Yang G, Liu Y, Li Y, Li J, Shen J, Chen Y, Wei Q (2020) Enhanced hydrogen absorption kinetics by introducing fine eutectic and long-period stacking ordered structure in ternary eutectic Mg–Ni–Y alloy. J Alloys Compd 820:153187

Stamatakis E, Zoulias E, Tzamalis G, Massina Z, Analytis V, Christodoulou C, Stubos A (2018) Metal hydride hydrogen compressors: current developments & early markets. Renew Energy 127:850–862

Suh MP, Park HJ, Prasad TK, Lim DW (2012) Hydrogen storage in metal–organic frameworks. Chem Rev 112(2):782–835

Sun D, Enoki H, Bououdina M, Akiba E (1999) Phase components and hydriding properties of the sintered Mg–xwt.% LaNi$_5$ (x= 20–50) composites. J Alloys Compd 282(1–2):252–257

Wagemans RW, van Lenthe JH, de Jongh PE, Van Dillen AJ, de Jong KP (2005) Hydrogen storage in magnesium clusters: quantum chemical study. J Am Chem Soc 127(47):16675–16680

Wang Y, Aizawa T, Nishimura C (2006) Solid-state synthesis of hydrogen storage Mg$_2$Co alloys via bulk mechanical alloying. Mater Trans 47(4):1052–1057

Wang J, Li HW, Chen P (2013) Amides and borohydrides for high-capacity solid-state hydrogen storage—materials design and kinetic improvements. MRS Bull 38(6):480–487

Wang H, Zhong H, Ouyang L, Liu J, Sun D, Zhang Q, Zhu M (2014) Fully reversible de/hydriding of Mg base solid solutions with reduced reaction enthalpy and enhanced kinetics. J Phys Chem C 118(23):12087–12096

Wang L, Rawal A, Aguey-Zinsou KF (2019) Hydrogen storage properties of nanoconfined aluminium hydride (AlH3). Chem Eng Sci 194:64–70

Wiberg E, Amberger E (1971) Hydrides of the elements of main groups I-IV. Elsevier Publishing Company

Xia Y, Yang Z, Zhu Y (2013) Porous carbon-based materials for hydrogen storage: advancement and challenges. J Mater Chem A 1(33):9365–9381

Xu C, Lin HJ, Wang Y, Zhang P, Meng Y, Zhang Y, Liu Y, Zhang J, Li L, Shi Q, Li W (2019) Catalytic effect of in situ formed nano-Mg$_2$Ni and Mg$_2$Cu on the hydrogen storage properties of Mg-Y hydride composites. J Alloy Compd 782:242–250

Yamaura SI, Kim HY, Kimura H, Inoue A, Arata Y (2002) Electrode properties of rapidly solidified Mg67Ni23Pd10 amorphous alloy. J Alloy Compd 347(1–2):239–243

Yang F, Meng X, Deng J, Wang Y, Zhang Z (2008) Identifying heat and mass transfer characteristics of metal hydride reactor during adsorption—parameter analysis and numerical study. Int J Hydrogen Energy 33(3):1014–1022

Zaluska A, Zaluski L, Ström-Olsen JO (2001) Structure, catalysis and atomic reactions on the nanoscale: a systematic approach to metal hydrides for hydrogen storage. Appl Phys A 72(2):157–165

Zhang J, Zhu Y, Lin H, Liu Y, Zhang Y, Li S, Ma Z, Li L (2017) Metal hydride nanoparticles with ultrahigh structural stability and hydrogen storage activity derived from microencapsulated nanoconfinement. Adv Mater 29(24):1700760

Zhang J, Li Z, Wu Y, Guo X, Ye J, Yuan B, Wang S, Jiang L (2019) Recent advances on the thermal destabilization of Mg-based hydrogen storage materials. RSC Adv 9(1):408–428

Zhao DL, Zhang YH (2014) Research progress in Mg-based hydrogen storage alloys. Rare Met 33(5):499–510

Zheng S, Fang F, Zhou G, Chen G, Ouyang L, Zhu M, Sun D (2008) Hydrogen storage properties of space-confined NaAlH$_4$ nanoparticles in ordered mesoporous silica. Chem Mater 20(12):3954–3958

Zhong HC, Wang H, Liu JW, Sun DL, Zhu M (2011) Altered desorption enthalpy of MgH_2 by the reversible formation of Mg (In) solid solution. Scripta Mater 65(4):285–287

Zhu M, Zhu WH, Chung CY, Che ZX, Li ZX (1999) Microstructure and hydrogen absorption properties of nano-phase composite prepared by mechanical alloying of MmNi5−x (CoAlMn) x and Mg. J Alloy Compd 293:531–535

Zhu M, Wang H, Ouyang LZ, Zeng MQ (2006) Composite structure and hydrogen storage properties in Mg-base alloys. Int J Hydrogen Energy 31(2):251–257

Züttel A, Wenger P, Rentsch S, Sudan P, Mauron P, Emmenegger C (2003) $LiBH_4$ a new hydrogen storage material. J Power Sources 118(1–2):1–7